Structural Evolution of SiO 2 Glass with Si Coordination Number Greater than 6

Article *in* Physical Review Letters · November 2020

DOI: 10.1103/PhysRevLett.125.205701

5 authors, including:

Yanbin Wang
University of Chicago
391 PUBLICATIONS **10,053** CITATIONS
SEE PROFILE

Guoyin Shen
Carnegie Institution for Science
378 PUBLICATIONS **11,160** CITATIONS
SEE PROFILE

Structural Evolution of SiO_2 Glass with Si Coordination Number Greater than 6

Yoshio Kono,[1,2,*] Yu Shu,[3] Curtis Kenney-Benson,[3] Yanbin Wang,[4] and Guoyin Shen[3]
[1]Geophysical Laboratory, Carnegie Institution of Washington, 9700 South Cass Avenue, Argonne, Illinois 60439, USA
[2]Geodynamics Research Center, Ehime University, 2-5 Bunkyo-cho, Matsuyama 790-8577, Japan
[3]High Pressure Collaborative Access Team, X-ray Science Division, Argonne National Laboratory, Argonne, Illinois 60439, USA
[4]GeoSoilEnviroCARS, Center for Advanced Radiation Sources, The University of Chicago, 5640 South Ellis Avenue, Chicago, Illinois 60637, USA

(Received 18 June 2020; accepted 11 September 2020; published 12 November 2020)

Pair distribution function measurement of SiO_2 glass up to 120 GPa reveals changes in the first-, second-, and third-neighbor distances associated with an increase in Si coordination number C_{Si} to >6 above 95 GPa. Packing fractions of Si and O determined from the first- and second-neighbor distances show marked changes accompanied with the structural evolution from $C_{Si} = 6$ to >6. Structural constraints in terms of ionic radius ratio of Si and O, and ratio of nonbonded radius to bonded Si—O distance support the structural evolution of SiO_2 glass with $C_{Si} > 6$ at high pressures.

DOI: 10.1103/PhysRevLett.125.205701

Knowledge of pressure-induced structural changes in network-forming glasses is of great interest in various scientific fields such as condensed matter physics, geophysics, materials science, and engineering. As a prototype network-forming glass, SiO_2 glass undergoes pressure-induced coordination number changes and has been the most extensively studied. It has been well known that the coordination number of Si [C_{Si}] in SiO_2 glass gradually increases from 4 to 6 at ~15–50 GPa [1–3]. However, further structural changes to $C_{Si} > 6$ at ultrahigh pressure conditions are controversial. Some simulation studies predicted $C_{Si} > 6$ above ~100 GPa in SiO_2 melt [4] and glass [5]. An earlier experimental work based on pair distribution function [$g(r)$] measurement reported that C_{Si} remains constant at 6 up to at least 102 GPa [2]. A kink in the pressure dependence of shear wave velocity was observed above ~140 GPa [6], which was interpreted as the formation of $C_{Si} > 6$ structural motifs. Recently, Ref. [3] succeeded in measuring $g(r)$ up to 172 GPa, and reported that C_{Si} continuously increases from 6 to 6.8 between 50 and 172 GPa. However, their C_{Si} versus pressure results [3] are inconsistent with previous reports [2,6], neither showing a stable plateau at $C_{Si} = 6$ with increasing pressure nor displaying an observable slope change in C_{Si} around 140 GPa. A more recent study [7] investigated structure of SiO_2 glass by a combination of x-ray diffraction and molecular dynamics (MD) simulations, and showed that C_{Si} remains at ~6 between 46 and 83 GPa and begins increasing to >6 above 109 GPa. Two x-ray Raman studies also give inconsistent results. One study, based on oxygen K-edge and silicon $L_{2,3}$-edge x-ray Raman spectroscopy up to 108 GPa and MD simulations up to 150 GPa, showed that average C_{Si} in SiO_2 glass remains lower than 6 at pressures up to 150 GPa [8]. Another oxygen K-edge spectroscopy study up to 160 GPa showed that coordination number of oxygen increases with pressure from 2 at ambient pressure to nearly 3.5 at 160 GPa [9]; in other words, the C_{Si} increases toward 7.

A clear determination of C_{Si} at ultrahigh pressure conditions is crucial not only for understanding the pressure-induced structural evolution of network-forming glasses but also for discussing the nature of magmas in the Earth's deep mantle (up to ~136 GPa) in geophysics. The discussions on changes in C_{Si} in Refs. [7,8] rely on MD simulations, while the results in Refs. [2,3] are solely based on *in situ* $g(r)$ measurements at ultrahigh pressure conditions. One possible cause of the inconsistency in the latter two experimental studies may be due to the accuracy in the $g(r)$ measurements, because of experimental challenges in the measurement of $g(r)$ at ultrahigh pressure conditions of >100 GPa. It has been reported that C_{Si} determined from x-ray structure factor [$S(Q)$] measurements with a limited range of momentum transfer (Q) of less than 12 $Å^{-1}$ can contain large uncertainties [10]. The maximum Q and pressure range in previous $g(r)$ measurements are 14 $Å^{-1}$ and 102 GPa [2], and 10 $Å^{-1}$ and 172 GPa [3], respectively.

In order to overcome the technical difficulties in accurate determination of $g(r)$, we utilized our recently developed opposed-anvil-type double-stage large-volume cell combined with multiangle energy dispersive x-ray diffraction [11–13] (cf. Supplemental Material [14]). The opposed-anvil-type double-stage large-volume cell is a recently developed high-pressure technique, enabling for significantly larger sample volume than those of diamond anvil cell experiments used in previous studies [2,3]. Use of

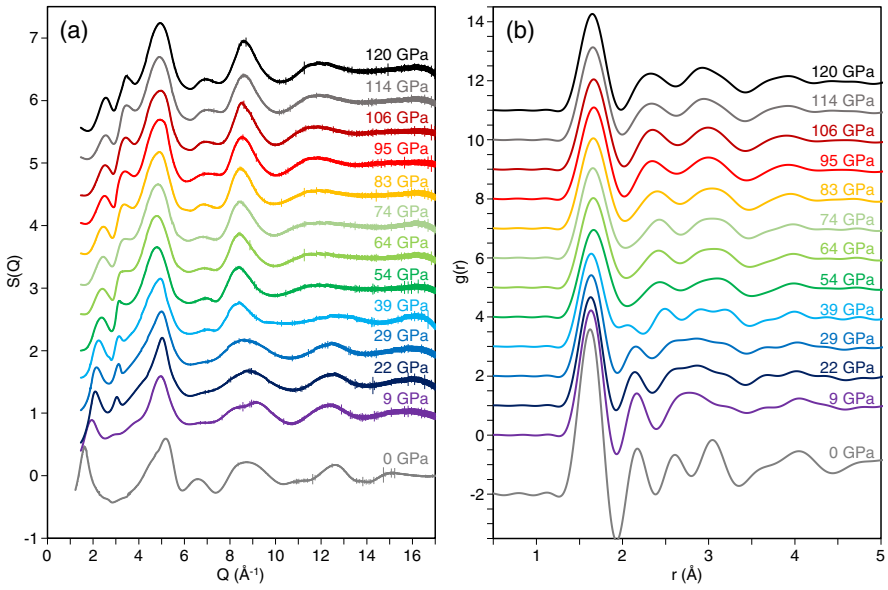

FIG. 1. Structure factor $[S(Q)]$ (a) and pair distribution function $[g(r)]$ (b) of SiO_2 glass up to 120 GPa. $S(Q)$ is displayed by a vertical offset of $+0.5$ for high-pressure data and of -1.0 for ambient pressure data. $g(r)$ is displayed by a vertical offset of $+1.0$ for high-pressure data and -2.0 for ambient pressure.

large-volume sample is beneficial to gain signal from weak x-ray scattering SiO_2 glass, and it allows for measuring $S(Q)$ with a large range of momentum transfer Q ($Q = 4\pi E \sin\theta/12.398$, where E is x-ray energy and θ is diffraction angle), which is essential to improve the resolution in real space in the $g(r)$.

Figure 1(a) shows $S(Q)$ of SiO_2 glass over a Q range up to 17 $Å^{-1}$ under the pressure conditions up to 120 GPa, with data quality remaining essentially unchanged up to the maximum pressure. With increasing pressure the $S(Q)$ spectra reveal the emergence of a new peak around 3 $Å^{-1}$ above 9 GPa, considered to represent formation of sixfold coordination species [2,7,18]. This peak becomes more predominant with increasing pressure. Figure 1(b) shows $g(r)$ of SiO_2 glass determined by Fourier transformation of the $S(Q)$ data. The $g(r)$ at ambient pressure shows somewhat negative values around the minimum near 1.9 Å, possibly due to the truncation effect in Fourier transformation. It is reported that Si—O, O—O, and Si—Si distances of SiO_2 glass at ambient pressure are 1.60 ± 0.01 Å, 2.62 ± 0.01 Å, and 3.08 ± 0.01 Å, respectively [19]. Our obtained first (r_1), second (r_2), and third (r_3) peaks in $g(r)$ (Supplemental Material, Table I [14]) agree with the literature. At pressures between 9 and 22 GPa, r_1 is similar to that at ambient pressure. It then increases rapidly from 1.622 Å at 22 GPa to 1.670 Å at 54 GPa (Fig. 2). At 54 GPa, r_1 is close to the Si—O distance of crystalline SiO_2 in the $CaCl_2$-type structure [20], indicating that SiO_2 glass now consists of octahedrally coordinated structural motif. As pressure continues to increase, r_1 remains similar to the Si—O distances of the corresponding crystalline SiO_2 phases (stishovite [21], $CaCl_2$-type [20], and α-PbO_2 type [20]). At ambient pressure, r_2 and r_3 observed in SiO_2 glass correspond to the average O—O distance in the SiO_4 tetrahedra and the Si—Si distance of corner-linked SiO_4 in quartz [22], respectively (Fig. 2). At 9–29 GPa, the r_2 and r_3 peaks exhibit partial overlap [Fig. 1(b)], probably because r_2 maintains the O—O distance of regular SiO_4 tetrahedra while the Si—Si distance (r_3) changes due to bending of the tetrahedral chain upon compression. Above 39 GPa, r_2 and r_3 separate again, primarily due to shortening of r_2. Above 54 GPa, r_2 and r_3 are similar to the O—O and longer Si—Si [labeled as $(Si-Si)_2$] distances of the crystalline SiO_2 phases (stishovite [21] and $CaCl_2$ type [20]), respectively (Fig. 2), suggesting that formation of octahedrally coordinated SiO_6 structure shortens O—O distance (r_2) in SiO_2 glass. Above 54 GPa, there is no observable peak in $g(r)$ around 2.6 Å, which is around the minimum between r_2 and r_3 [Fig. 1(b)] and corresponds to the shorter Si—Si distance [$(Si—Si)_1$] in the crystalline SiO_2 phases (stishovite [21] and $CaCl_2$ type [20]). In crystalline $CaCl_2$-type SiO_2, there are eight $(Si—Si)_2$ distances and only two $(Si—Si)_1$ distances. We therefore attribute the absence of the $(Si—Si)_1$ peak in SiO_2 glass at high pressures to the absence or low population of $(Si—Si)_1$ distances similar to the crystalline phases at similar pressures. The r_2 peak of SiO_2 glass remains essentially constant between 54 and 83 GPa, while it decreases again with pressure above 83 GPa (Fig. 2).

We determine C_{Si} in SiO_2 glass based on the area under the r_1 peak in $g(r)$. We first derive pseudopartial correlation function of Si—O $[T(r)_{Si-O}]$ according to Ref. [3]

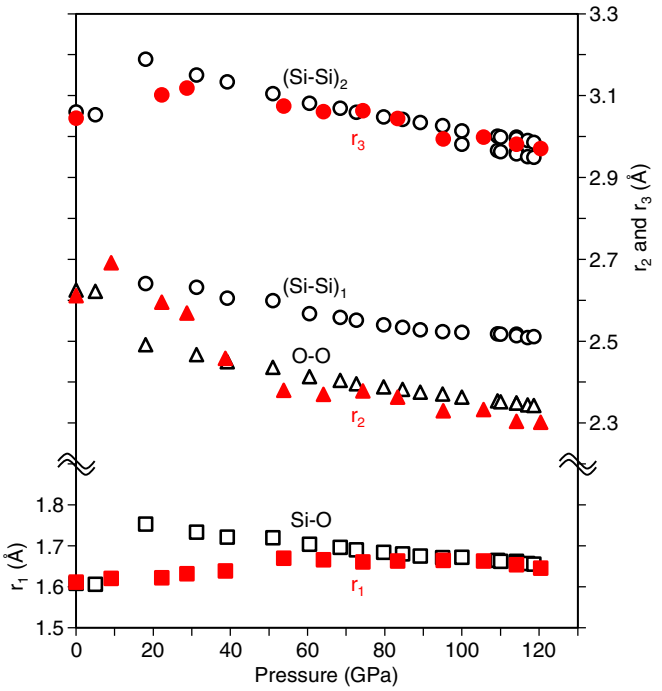

FIG. 2. The first (r_1), second (r_2), and third (r_3) peak positions in $g(r)$ of SiO_2 glass. Solid red symbols represent the r_1, r_2, and r_3 of SiO_2 glass, and open black symbols are average Si—O (squares), O—O (triangles), and Si—Si (circles) distances of crystalline SiO_2 (quartz at 0–5 GPa [22], stishovite at 18–39 GPa [21], $CaCl_2$ type at 51–95 GPa [20], α-PbO_2 type at 100–119 GPa [20]) calculated by using lattice parameters at high pressures [23].

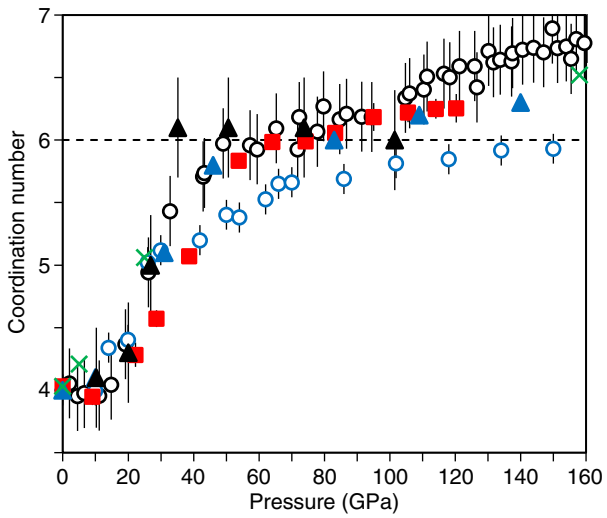

FIG. 3. Si coordination number in SiO_2 glass. Solid red squares: this study, solid black triangles [2], open black circles [3], solid blue triangles [7], and open blue circles [8]. Green crosses are Si coordination number of SiO_2 melt calculated by first-principles simulation [4].

(cf. Supplemental Material [14]). Since our measurements of $S(Q)$ were collected with a large Q range up to 17 $Å^{-1}$, $T(r)_{Si-O}$ shows well-separated Si—O peaks (Supplemental Material, Fig. S1 [14]), which effectively removes the uncertainty due to the overlap with the O—O peak as discussed in previous study [3]. Figure 3 compares C_{Si} determined in this study with those reported in previous studies [2,3,7,8]. The corresponding values are summarized in Supplemental Material, Table I [14]. Our results show that C_{Si} remains around 4 below 10 GPa, increases gradually to 6 between 10 and 54 GPa, stays near constant at 6 between 54 and 83 GPa, and finally becomes greater than 6 above 95 GPa.

Our observed C_{Si} evolution is in reasonable agreement with the results of four previous studies [2,3,7,9] (Fig. 3). Reference [2] reported that C_{Si} increases to ~6 at 35 GPa, and C_{Si} stays at ~6 above 35 GPa until 102 GPa. Similarly, Ref. [7] also shows C_{Si} of ~6 at 46 and 83 GPa, and >6 above 109 GPa (Fig. 3). The C_{Si} values of Ref. [3] are also similar to this study. Within the reported uncertainties, their results can be interpreted as having a plateau of $C_{Si} = 6$ up to ~100 GPa (Fig. 3). Above ~106 GPa, the C_{Si} values of Ref. [3] clearly exceed 6, consistent with this study. In addition, we note that a recent x-ray Raman study shows evolution of heavily contracted oxygen environments characterized by a decrease in average O—O distance and emergence of fourfold coordinated oxygen above 100 GPa [9]. The average oxygen coordination number exceeding 3 above 100 GPa [9] means C_{Si} greater than 6, which is consistent with our observations. Combining data from this study and the four previous reports [2,3,7,9], we conclude that C_{Si} increases to ~6 between 35 and 54 GPa and stays more or less constant at ~6 up to ~100 GPa. Then, C_{Si} increases to more than 6 above ~100 GPa (Fig. 3). Only one study [8] reported C_{Si} lower than 6 at pressures up to 150 GPa. However, we note that, although the average C_{Si} values are somewhat lower than those of the above studies, the MD simulations reported by these authors show that population of $C_{Si} = 7$ species begins increasing above 110 GPa [8].

Several recent studies have discussed oxygen packing fraction (OPF) as a geometric parameter to understand evolution of coordination number in oxide glasses [3,7,11,24]. However, geometric factor for the structural evolution from $C_{Si} = 6$ to >6 has not been well understood. Figure 4(a) shows the packing fractions of oxygen (OPF) and silicon (SiPF) of SiO_2 glass above 54 GPa, where C_{Si} is ~6 or higher. The OPF and SiPF values are derived from r_1 (Si—O distance) and r_2 (O—O distance) obtained in this study with the density data of SiO_2 glass from Ref. [25] (cf. Supplemental Material [14]). It is important to note that, in previous studies, radius of oxygen (r_O) is estimated from r_1 (Si—O distance) by assuming octahedral geometry for $C_{Si} = 6$ (Ref. [24]) and Fe_2P-type structure with effective $C_{Si} = 8.5$ (Ref. [3]) as the end member for $C_{Si} > 6$. In this study, we derive r_O directly from measured r_2, which provides direct information for the behavior of OPF with increasing pressure. The results show that OPF increases with pressure when C_{Si} is ~6, which is consistent with previous studies [11,24]. However, OPF turns around and

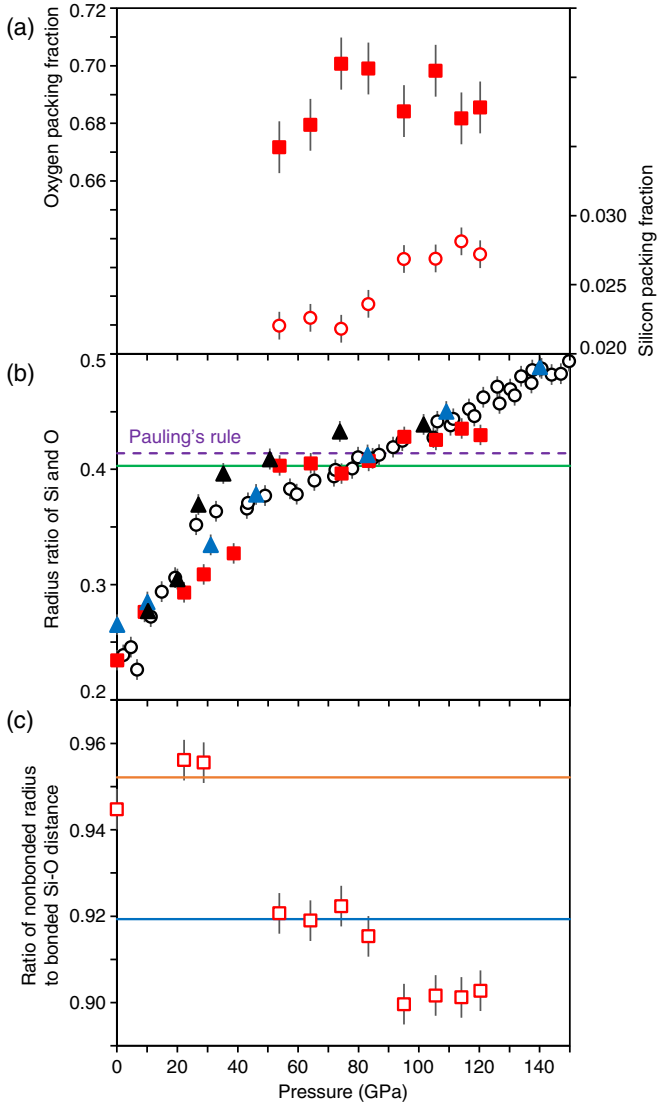

FIG. 4. (a) Oxygen (solid squares) and silicon (open circles) packing fraction of SiO_2 glass. (b) Radius ratio of Si and O, calculated from all the existing Si—O distance data (solid red squares: this study, solid black triangles [2], open black circles [3], solid blue triangles [7]). (c) Ratio of nonbonded radius to bonded Si—O distance.

starts to decreases above 95 GPa [Fig. 4(a)], where the C_{Si} clearly exceeds 6. In contrast, SiPF remains almost constant between 54 and 83 GPa, where C_{Si} is ~6, and then increases above 95 GPa [Fig. 4(a)]. The change of SiPF above 83 GPa (9.7×10^{-5}/GPa) is ~2.5 times higher than that at 54–83 GPa (3.9×10^{-5}/GPa). The decrease in OPF and the steep increase in SiPF clearly indicate a relative increase in ionic radius of silicon due to the increase of C_{Si} to >6 above 95 GPa. These packing fractions, which are based on directly measured r_1 and r_2 distances, may be viewed as more robust indicators for the structural change from $C_{Si} = 6$ to >6 in SiO_2 glass without having to rely on the determination of C_{Si}, which may be complicated by possible overlaps in the Si—O and O—O peaks in $g(r)$ [3].

The principle of determining coordinated polyhedron structures in view of atomic radii is known as Pauling's rule in crystalline systems [26], where coordination number of a cation in contact with a given number of anions with the shape of a coordinated polyhedron is rationalized by the ratio of the radius of the cation (Si) to that of the anion (O), $\gamma(\mathrm{Si/O})$. Figure 4(b) shows $\gamma(\mathrm{Si/O})$ of SiO_2 glass as a function of pressure. Over a wide pressure range of ~50 to ~90 GPa, C_{Si} remains essentially constant at ~6, and our obtained $\gamma(\mathrm{Si/O})$ is also almost constant at 0.403 ± 0.004 [green line in Fig. 4(b)], which is close to the minimum radius ratio of octahedral polyhedron according to Pauling's rule (0.414) [purple line in Fig. 4(b)]. Above 95 GPa, $\gamma(\mathrm{Si/O})$ begins to increase to greater than 0.403, which coincides with a modification of the Si—O polyhedron along with the increase of C_{Si} to >6.

We have calculated the $\gamma(\mathrm{Si/O})$ values from the literature data based on x-ray diffraction [2,3,7] by using the reported Si—O distances and our observed r_O values at 1 bar and 54–120 GPa, based on a linear regression ($r_O = -1.182 \times 10^{-3} \times P + 1.281$, where P is pressure in GPa). The calculated $\gamma(\mathrm{Si/O})$ from Ref. [2,3,7] are consistent with our data. In particular, it is important to note that all the calculated $\gamma(\mathrm{Si/O})$ values of this study and previous studies [2,3,7] show a consistent behavior above ~90 GPa [Fig. 4(b)], which implies consistency in the local structural change among this study and previous studies in view of $\gamma(\mathrm{Si/O})$, despite the reported discrepancies in C_{Si}. The discrepancy in C_{Si} may be attributed to the details of calculations in the determination of C_{Si} (area of the Si—O peak) because of possible overlaps in the Si—O and O—O peaks as discussed in Ref. [3]. The consistent behavior in the evolution of $\gamma(\mathrm{Si/O})$ among this study and previous studies [2,3,7], all of which are determined from the Si—O distance (peak position) in the $g(r)$, strongly suggests that a structural change from $C_{Si} = 6$ to >6 takes place above ~95 GPa.

Reference [27] proposes an alternative approach to describe structural units by the ratio of nonbonded Si radius (R) to bonded Si—O distance (r_1), by considering the number of cations (Si) surrounding an anion (O). Simple geometric arguments show that for corner-shared one-angle configuration at ambient pressure, R/r_1 is ≤1.000 for OSi_2, ≤0.866 for OSi_3, and ≤0.816 for OSi_4 [27]. Following Ref. [27], we calculated nonbonded radius in SiO_2 glass from r_3 (the Si—Si distance) by $R = r_3/2$. R/r_1 shows high values of 0.945–0.956 at 0–29 GPa [orange line in Fig. 4(c)], where $C_{Si} = \sim 4$ (i.e., OSi_2), and decreases rapidly to 0.921 at 54 GPa, indicative of a coordination change from OSi_2 to OSi_3 (i.e., SiO_6) similar to crystalline stishovite [27]. Our R/r_1 value at 54 GPa is somewhat higher than that predicted for OSi_3 at ambient pressure [27]. The discrepancy may be due to possible existence of edge-shared two-angle configuration and/or minor amount of shorter $(\mathrm{Si—Si})_1$ distance in SiO_2 glass as predicted in MD

and *ab initio* simulations [7,28]. R/r_1 stays nearly constant (0.922–0.915) between 54 and 83 GPa [blue line in Fig. 4(c)], indicating a stable structural configuration. Above 95 GPa, R/r_1 decreases sharply again, implying further structural change. A recent MD simulation predicted formation of OSi_4 in SiO_2 glass between 83 and 140 GPa [7], consistent with our observed decrease of R/r_1 above 95 GPa. It is important to note the consistency between the ionic radius ratio model [Fig. 4(b)] and the nonbonded radius model [Fig. 4(c)]. Both $\gamma(\mathrm{Si/O})$ and R/r_1 change rapidly between 29 and 54 GPa followed by a stable plateau at 54–83 GPa, considered as structural change in space filling structure from OSi_2 to OSi_3 and polyhedron structure from SiO_4 to SiO_6. Then, above 95 GPa, both $\gamma(\mathrm{Si/O})$ and R/r_1 change again simultaneously (Fig. 4), indicating further structural change in SiO_2 glass to $C_{Si} > 6$.

Our results of the structural evolution of SiO_2 glass to $C_{Si} > 6$ above 95 GPa provide important implications not only for understanding the mechanism of the pressure-induced structural evolution of network-forming glasses in physics and materials sciences but also for discussing nature of silicate magmas in geophysics. It has been known that structural change from $C_{Si} = 4$ to 6 in silicate melt occurs at pressure conditions similar to that of SiO_2 glass [29,30]. Our data on SiO_2 glass imply that structural change to $C_{Si} > 6$ may also occur in silicate melts at pressures above ~95 GPa. In fact, first-principles simulations gave C_{Si} of 6.52 in SiO_2 melt at ~158 GPa and 6000 K [4]. Such a C_{Si} value is similar to that of SiO_2 glass reported here (Fig. 3) and in Ref. [3]. Although evolution of average C_{Si} may vary between SiO_2 and more complex silicate compositions, several first-principles molecular dynamics simulations (e.g., basalt liquid [31]; $MgSiO_3$ liquid [32]; and glass [33]) report the occurrence of sevenfold coordination species above ~100 GPa. At room temperature and at 110 GPa, a density of SiO_2 glass of 5.27 ± 0.13 g/cm^3 [25] is identical, within measurement errors, to that of $CaCl_2$-type crystalline SiO_2 with $C_{Si} = 6$ structure (5.31 g/cm^3) [34]. First-principles simulations show that density of SiO_2 melt exceeds that of α-PbO_2-type SiO_2 crystal with $C_{Si} = 6$ structure (seifertite) at ~120 GPa and 3000 K [4]. Since silicate minerals all have $C_{Si} = 6$ structures throughout the Earth's lower mantle (up to ~136 GPa), silicate melts with $C_{Si} > 6$ structure may become denser than the surrounding mantle minerals at deep mantle conditions, making it possible for deep magma ocean to be gravitationally stable.

We acknowledge two anonymous reviewers for constructive comments. We thank Ross Hrubiak and Changyong Park for the help in data analysis. This research is supported by the National Science Foundation under Grant No. EAR-1722495. High-pressure experiments were performed at HPCAT (Sector 16), Advanced Photon Source (APS), Argonne National Laboratory. HPCAT operations are supported by DOE-NNSA's Office of Experimental Sciences. The Advanced Photon Source is a U.S. Department of Energy (DOE) Office of Science User Facility operated for the DOE Office of Science by Argonne National Laboratory under Contract No. DE-AC02-06CH11357. Y. K. acknowledges support by JSPS KAKENHI Grants No. 19KK0093 and No. 20H00201, and by JSPS Bilateral Program Grant No. JPJSBP120209926. Y. W. acknowledges NSF support EAR-1620548.

*Corresponding author.
kono.yoshio.rj@ehime-u.ac.jp
Present address: Geodynamics Research Center, Ehime University, 2-5 Bunkyo-cho, Matsuyama 790-8577, Japan.

[1] C. J. Benmore, E. Soignard, S. A. Amin, M. Guthrie, S. D. Shastri, P. L. Lee, and J. L. Yarger, Phys. Rev. B **81**, 054105 (2010).
[2] T. Sato and N. Funamori, Phys. Rev. B **82**, 184102 (2010).
[3] C. Prescher, V. B. Prakapenka, J. Stefanski, S. Jahn, L. B. Skinner, and Y. Wang, Proc. Natl. Acad. Sci. U.S.A. **114**, 10041 (2017).
[4] B. B. Karki, D. Bhattarai, and L. Stixrude, Phys. Rev. B **76**, 104205 (2007).
[5] V. V. Brazhkin, A. G. Lyapin, and K. Trachenko, Phys. Rev. B **83**, 132103 (2011).
[6] M. Murakami and J. D. Bass, Phys. Rev. Lett. **104**, 025504 (2010).
[7] M. Murakami, S. Kohara, N. Kitamura, J. Akola, H. Inoue *et al.*, Phys. Rev. B **99**, 045153 (2019).
[8] S. Petitgirard *et al.*, Geochem. Perspect. Lett. **9**, 32 (2019).
[9] S. K. Lee, Y.-H. Kim, Y. S. Yi, P. Chow, Y. Xiao, C. Ji, and G. Shen, Phys. Rev. Lett. **123**, 235701 (2019).
[10] A. J. Leadbetter and A. C. Wright, J. Non-Cryst. Solids **7**, 141 (1972).
[11] Y. Kono, C. Kenney-Benson, D. Ikuta, Y. Shibazaki, Y. Wang, and G. Shen, Proc. Natl. Acad. Sci. U.S.A. **113**, 3436 (2016).
[12] Y. Kono, Y. Shibazaki, C. Kenney-Benson, Y. Wang, and G. Shen, Proc. Natl. Acad. Sci. U.S.A. **115**, 1742 (2018).
[13] Y. Kono, C. Kenney-Benson, and G. Shen, High Press. Res. **40**, 175 (2020).
[14] See Supplemental Material at http://link.aps.org/supplemental/10.1103/PhysRevLett.125.205701 for descriptions of opposed-type double-stage large-volume cell experiment and pair distribution function measurement, which includes Refs. [15–17], Supplemental Fig. S1 and Supplemental Table I.
[15] Y. Kono, C. Park, C. Kenney-Benson, G. Shen, and Y. Wang, Phys. Earth Planet. Inter. **228**, 269 (2014).
[16] G. Shen, V. B. Prakapenka, M. L. Rivers, and S. R. Sutton, Rev. Sci. Instrum. **74**, 3021 (2003).
[17] D. Pickup, R. Moss, and R. Newport, J. Appl. Crystallogr. **47**, 1790 (2014).
[18] C. Meade, R. J. Hemley, and H. K. Mao, Phys. Rev. Lett. **69**, 1387 (1992).
[19] Q. Mei, C. J. Benmore, S. Sen, R. Sharma, and J. L. Yarger, Phys. Rev. B **78**, 144204 (2008).

[20] D. M. Teter, R. J. Hemley, G. Kresse, and J. Hafner, Phys. Rev. Lett. **80**, 2145 (1998).
[21] T. Yamanaka, T. Fukuda, and J. Mimaki, Phys. Chem. Miner. **29**, 633 (2002).
[22] J. D. Jorgensen, J. Appl. Phys. **49**, 5473 (1978).
[23] B. Grocholski, S. H. Shim, and V. B. Prakapenka, J. Geophys. Res. **118**, 4745 (2013).
[24] A. Zeidler, P. S. Salmon, and L. B. Skinner, Proc. Natl. Acad. Sci. U.S.A. **111**, 10045 (2014).
[25] S. Petitgirard *et al.*, Phys. Rev. Lett. **119**, 215701 (2017).
[26] L. Pauling, J. Am. Chem. Soc. **51**, 1010 (1929).
[27] M. O'Keeffe and B. G. Hyde, Struct. Bond. Cryst. **1**, 227 (1981).
[28] N. Li, R. Sakidja, S. Aryal, and W.-Y. Ching, Phys. Chem. Chem. Phys. **16**, 1500 (2014).
[29] C. Sanloup, J. W. E. Drewitt, Z. Konôpková, P. Dalladay-Simpson, D. M. Morton, N. Rai, W. van Westrenen, and W. Morgenroth, Nature (London) **503**, 104 (2013).
[30] C. Sanloup, Chem. Geol. **429**, 51 (2016).
[31] S. Bajgain, D. B. Ghosh, and B. B. Karki, Nat. Commun. **6**, 8578 (2015).
[32] L. Stixrude and B. Karki, Science **310**, 297 (2005).
[33] D. B. Ghosh, B. B. Karki, and L. Stixrude, Am. Mineral. **99**, 1304 (2014).
[34] D. Andrault, R. J. Angel, J. L. Mosenfelder, and T. Le Bihan, Am. Mineral. **88**, 301 (2003).